

Article

Erosion and Sedimentation Processes in a Semi-Arid Basin of the Brazilian Savanna under Different Land Use, Climate Change, and Conservation Scenarios

Bianca Pietsch Cunha Bendito ^{1,*}, Henrique Marinho Leite Chaves ¹  and Aldicir Scariot ² 

¹ Forestry Department, University of Brasilia—UnB, Brasilia 70910-900, DF, Brazil

² Embrapa Genetic Resources and Biotechnology, Laboratory of Ecology and Conservation, Brasilia 70770-917, DF, Brazil

* Correspondence: biancabenditoo@gmail.com

Abstract: Estimating the on-site and off-site impacts of soil erosion as a function of land use and climate conditions in semi-arid basins is key for soil and water conservation strategies. However, a research gap exists in the theme, requiring further investigation using local hydrological data. To accomplish it, the SDR-InVEST model was applied to the Pardo-FB basin (Brazil) using different land use, soil conservation, and climate conditions. The mean annual soil loss and the mean sediment yield in the basin varied between 7 and 36 Mg ha⁻¹ yr⁻¹ and 1.2 and 52.2 Gg yr⁻¹, respectively. The basin areas where on-site and off-site erosion tolerances were exceeded ranged from 20% to 50% and from 0% to 1%, respectively, depending on the scenario. The results indicate that anthropic areas and high erosivities increase soil detachment and decrease sediment retention, generating higher erosion and sedimentation rates in the basin. The restoration of native vegetation and soil conservation practices reduced the erosion impacts, but their effectiveness was reduced in the wet climate scenario. The results contribute to the establishment of soil conservation strategies in the Pardo basin, as well as in similar basins around the world.



Citation: Bendito, B.P.C.; Chaves, H.M.L.; Scariot, A. Erosion and Sedimentation Processes in a Semi-Arid Basin of the Brazilian Savanna under Different Land Use, Climate Change, and Conservation Scenarios. *Water* **2023**, *15*, 563.
<https://doi.org/10.3390/w15030563>

Academic Editor: Yeshuang Xu

Received: 5 December 2022

Revised: 19 January 2023

Accepted: 22 January 2023

Published: 1 February 2023



Copyright: © 2023 by the authors. Licensee MDPI, Basel, Switzerland. This article is an open access article distributed under the terms and conditions of the Creative Commons Attribution (CC BY) license (<https://creativecommons.org/licenses/by/> 4.0/).

Keywords: InVEST model; land use; climate variability; semi-arid savanna

1. Introduction

Humans rely heavily on the ability of soils to sustain agricultural production and livestock [1]. At the same time, agricultural systems, along with climate change, are the main drivers of soil degradation [2]. Hydrological alterations, such as increased rainfall intensity caused by climate change, can further accelerate this process [3]. Therefore, tools that go beyond the simple diagnosis of soil erosion and are able to evaluate the effectiveness of mitigation strategies in future climate scenarios are urgently needed. Distributed soil erosion modeling has filled this gap, which allows the spatial assessment of soil erosion and land degradation and provides the necessary technical and political visibility to warrant effective soil conservation policies [4,5].

In the tropics, the risk of soil erosion is potentially high due to natural factors, such as high rain erosivity and soil erodibility, with soil loss frequently exceeding 20 Mg ha⁻¹ yr⁻¹ [1]. In Brazil, the mean annual soil loss ranges from 0.1 Mg ha⁻¹ yr⁻¹, under permanent cover conditions, to 136.0 Mg ha⁻¹ yr⁻¹, under conventional agriculture [6]. The recent agricultural expansion in the Brazilian savanna has caused significant economic and environmental costs [3,6,7]. In that region, the high erosion rates, often surpassing soil loss tolerances, are strongly associated with non-permanent soil cover and highly erodible soils [8].

Although land cover and management practices play an important role in the control of soil erosion, the relationship is not yet fully understood in semiarid regions of the Brazilian Cerrado [6,7,9], particularly under a changing climate [3,10–12]. Such is the

case of the Pardo River basin in southeastern Brazil, whose climate, geomorphology, and pedology favor soil erosion and degradation [13].

The combined impacts of LULC and climate on on-site erosion include reductions in crop productivity [7] and increased soil degradation [1]. Tolerable on-site erosion is a soil loss threshold that still maintains its production and ecological functions, including agronomic sustainability. In the United States and Europe, on-site tolerance is related to a loss of productivity, ranging between 5 and 12 Mg ha⁻¹ year⁻¹ [14,15]. In Brazil, it varies from 2 to 15 t ha⁻¹ yr⁻¹, depending on soil depth and texture [16].

The sediments eroded upstream are transported downstream, generating off-site impacts such as silting and water quality impairment [17–19]. Off-site soil loss tolerance is lower than on-site thresholds and is usually taken as 1.0 Mg ha⁻¹ year⁻¹ [18–20]. Both on- and off-site impacts should be accounted for, especially in semi-arid regions where soils are fragile and water resources are scarce [11]. Although studies have investigated off-site impacts in the Cerrado, such as sedimentation [21,22], its wide distribution following land conversion and climate change requires more investigation [10,23].

Spatially-distributed erosion modeling has been utilized to evaluate the on- and off-site impacts of soil loss [5,24]. However, many models, such as SWAT, WEPP, LISEM, and EUROSEM [4], are complex and require specialized knowledge and a high investment of time, limiting the number of potential users [4]. LISEM, EUROSEM, and SWAT require large amounts of detailed data and a large number of parameters, which hinders their application in data-scarce areas of developing countries. The WEPP is considered less accurate in areas that are less disturbed and dominated by vegetation, and, due to the non-linearity of the model, it has a strong propagation of errors in the results [25,26].

Simple yet robust models, such as the SDR-InVEST [27] bridge this gap [28]. Contrary to the other models, the SDR-InVEST model requires readily available data and low modeling skills. Furthermore, the model is based on the Universal Soil Loss Equation (USLE), which has intrinsic predictive limitations but relatively good accuracy [23,29–35]. Although the SDR-InVEST has been applied globally, with variable degrees of success, no studies were carried out in semi-arid savannas of Brazil [10,23]. Therefore, considering the importance of understanding the on-site and off-site impacts of erosive processes and their control in the Pardo river basin under present and prospective land use and climate change scenarios, the objectives of this study are: (1) to assess the distribution and severity of soil loss under the present land use conditions; (2) to quantify the corresponding sediment yield at the basin outlet; and (3) to evaluate the impact of land use change and climate variability on soil loss and sediment yield in the basin.

2. Materials and Methods

2.1. Study Area

The study area here called Pardo-FB, is in the Rio Pardo Basin, north of the state of Minas Gerais (MG) (Brazil), between latitudes S 15°0'42.595" and 15°51'9684" and longitudes O 42°31'9.304" and 42°30'39.337" (Figure 1). The Pardo-FB has an area of 5508 km² and includes five municipalities (Indaiabira, Montezuma, Rio Pardo de Minas, Santo Antônio do Retiro, and Vargem Grande do Rio Pardo) [36].

The basin climate is semi-arid [39], with a mean annual precipitation of 748 mm (Figure 2). The basin's relatively low rainfall and high temperature make it susceptible to desertification [39].

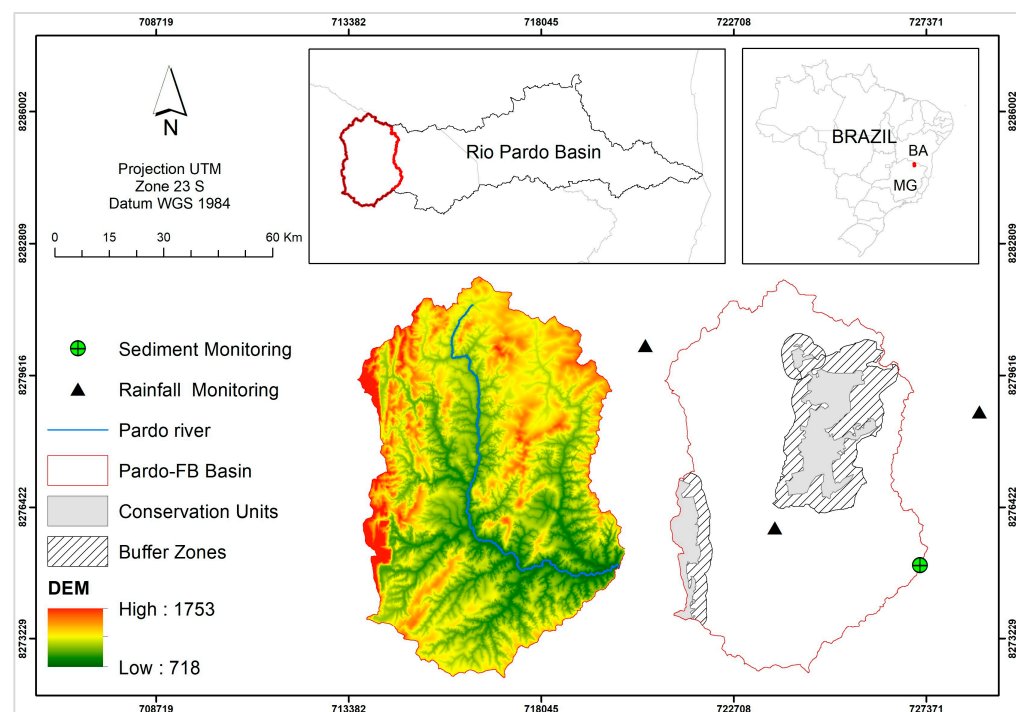


Figure 1. Location of the Pardo-FB Basin with principal watercourse (Pardo river); Digital Elevation Model (DEM); rainfall and sediment monitoring stations and Conservation Units Reserve for Sustainable Development “Nascentes Geraizeiras” (RDSNG); Montezuma State Park (PEM); and the “Serra Nova” e “Talhado” State Park (PESNT). The Pardo-FB basin has a mean altitude of 926 m and a mean slope of 13%. The basin is relatively circular in shape, with a compactness coefficient, shape factor, and circularity index of 1.43, 0.27, and 0.47, respectively. The drainage density is 1.23 km^{-1} , which provides a relatively fast runoff response to precipitation [37]. The predominant soils in the basin are Oxisols (55%), followed by Leptsols (20%) [38].

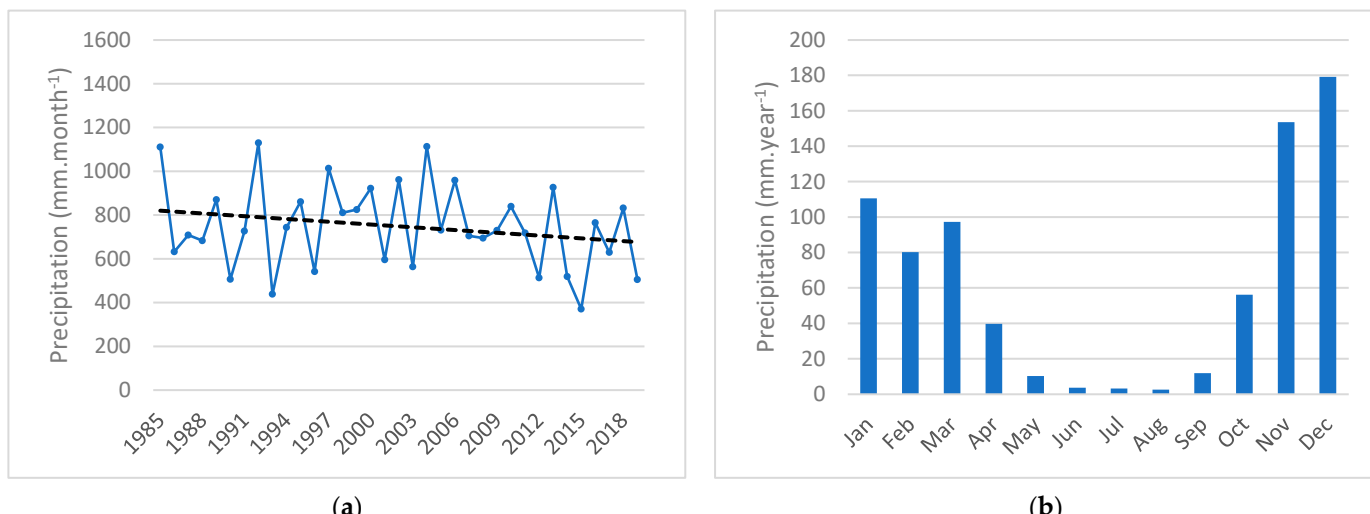


Figure 2. Annual rainfall (a) and mean monthly rainfall (b) in the Pardo-FB basin.

The Pardo-FB basin is predominantly covered by native savanna vegetation (Cerrado) (79%), and anthropized areas are occupied mostly by silviculture, pasture, and agriculture. The eucalyptus plantations were the main land use conversion in recent years in the basin [40].

As a response to social pressures against land use conversion in the basin, the Reserve for Sustainable Development “Nascentes Geraizeiras” (RDSNG) was created in 2014

(Figure 1). The other Conservation Units (UC) in the Pardo-FB basin are the Montezuma State Park (PEM) and the Serra Nova e Talhado State Park (PESNT), both fully protected conservation UCs.

2.2. Mean Annual Sediment Yield in the Basin

The observed daily sediment load at the basin outlet was the sum of the suspended load and the bed load, namely [37]:

$$Q_{st} = Q_{sm} + Q_{snm} \quad (1)$$

where Q_{st} is the total sediment load ($Mg\ d^{-1}$); Q_{sm} is the measured (suspended) sediment load ($Mg\ d^{-1}$); and Q_{snm} = unmeasured (bed) sediment load ($Mg\ d^{-1}$).

The observed sediment concentration (C_{ss}) and streamflow (Q) data, between 1997 and 2010, were obtained from the National Water and Sanitation Agency [41] at the Fazenda Benfica gaging station (no. 53490000) (Figure 1), situated at the basin outlet. The C_{ss} ($mg\ L^{-1}$) was converted into a measured (suspended) sediment load (Q_{sm} , $ton\ day^{-1}$) with the formula [37]:

$$Q_{sm} = 0.0864 \cdot Q \cdot C_{ss} \quad (2)$$

where Q is the daily streamflow ($m^3\ s^{-1}$); C_{ss} is the observed concentration of suspended solids ($mg\ L^{-1}$), 0.0864 = dimensionless coefficient for unit conversion [37].

The unmeasured bed load (Q_{snm}) was estimated from the measured suspended load (Q_{sm}), using a previously calibrated equation obtained for the Cerrado region of Brazil [37]:

$$Q_{snm} = 5.4 \cdot Q_{sm}^{0.638} \quad (3)$$

The sediment rating curve (SRC) was developed to estimate the annual average sediment on the basin outlet from the streamflow measurements. A SRC is the function that relates the measured streamflow (Q, $m^3\ s^{-1}$) and the sediment yield (Q_{st} , $ton\ day^{-1}$ or $kg\ s^{-1}$) by using regression analysis; usually the curve is expressed in the form of a power equation, with the R2 used as a goodness-of-fit index [37,42]:

$$Q_{st} = a \cdot Q^b \quad (4)$$

where Q_{st} is the sediment yield ($g\ s^{-1}$); Q is the streamflow ($m^3\ s^{-1}$); a & b = equation parameters [42]. The average daily sediment load was estimated using the SRC equation and the daily mean streamflow. The daily sediment loads are then calculated for the mean annual sediment load ($ton\ day^{-1}$) used in the model calibration.

2.3. InVEST Sediment Delivery Ratio Model

The SDR-InVEST is a distributed model that calculates the yearly soil loss in basin slopes, the annual sediment yield at the basin outlet, and the sediment retention resulting from a given land cover [27]. The mean annual soil loss for each basin pixel in the model is [43]:

$$USLE_i = R_i \cdot K_i \cdot LS_i \cdot C_i \cdot P_i \quad (5)$$

where $USLE_i$ is soil loss ($Mg\ ha^{-1}\ yr^{-1}$); R_i is rainfall erosivity ($MJ \cdot mm(ha \cdot hr \cdot yr)^{-1}$); K_i is soil erodibility ($Mg \cdot ha \cdot hr$ ($MJ \cdot ha \cdot mm$) $^{-1}$); LS_i is a slope length-gradient factor (unitless); C_i is a cover-management factor (unitless); and P is a support practice factor (unitless).

The LS_i is computed using the equation developed by Desmet and Govers [44]:

$$LS_i = S_i \frac{(A_{i-in} + D^2)^{m+1} - A_{i-in}^{m+1}}{D^{m+2} \cdot x_i^m \cdot (22.13)^m} \quad (6)$$

where S_i is the slope factor for grid cell i; A_{i-in} is the contributing area (m^2) at the inlet of a grid cell computed from the Multiple-Flow Direction method; D is the cell linear

dimension (m); x_i is the mean slope aspect weighted by proportional outflow from grid cell i ; m is the RUSLE slope length exponent factor. To avoid overestimation of the LS factor in heterogeneous landscapes, long slope lengths are capped at a maximum value that is adjustable as a user parameter (item 2.5) [44].

To compute the sediment yield in each pixel, the model uses the sediment delivery ratio-SDR, which is a function of the hydrological connectivity of the basin [45]

$$SDR_i = \frac{SDR_{max}}{1 + \exp\left(\frac{IC_0 - IC_i}{k}\right)} \quad (7)$$

where SDR_i is the sediment delivery ratio (unitless); SDR_{max} is the maximum theoretical SDR (unitless) [45]; IC_i is the connectivity index (unitless); and IC_0 and k are calibration parameters that define the shape of the $SDR-IC_0$ function (unitless).

The connectivity index (IC) is a pixel-by-pixel routing index based on the relationship between the slope and land use/land cover (LULC) of neighboring pixels, developed by Borselli et al. [46]:

$$IC = \log_{10}\left(\frac{D_{up}}{D_{dn}}\right) \quad (8)$$

$$D_{up} = \bar{C} \cdot \bar{S} \sqrt{A} \quad (9)$$

$$D_{dn} = \sum_i \frac{d_i}{C_i \cdot S_i} \quad (10)$$

where D_{up} is the upstream connectivity; D_{dn} is the downstream connectivity; \bar{C} is the average C factor of the upstream contributing area; \bar{S} is the average slope gradient of the upstream contributing area ($m m^{-1}$); A is the upstream contributing area (m^2); d_i is the length of the flow path in the steepest downslope direction (m); and C_i and S_i are the C and the S factor of the its pixel, respectively.

The sediment yield that reaches the basin outlet is [27]:

$$E_i = USLE_i \cdot SDR_i \quad (11)$$

$$E_{sim} = \sum E_i \quad (12)$$

where E_i is the sediment export from a given pixel i ($Mg ha^{-1} yr^{-1}$); $USLE_i$ is the soil loss ($Mg ha^{-1} yr^{-1}$); SDR_i is the sediment delivery ratio (unitless); and E_{sim} is the total catchment sediment export.

Sediment retention (Ret_i) represents the avoided soil loss provided by the current land use, weighted by the SDR factor. It is estimated by the difference between the amount of sediment exported under the present land cover (LULC) and the amount of sediment exported in the bare soil condition [27]:

$$Ret_i = (RKLS_i \cdot SDR_{bar}) - E_i \quad (13)$$

where Ret_i = sediment retention in the pixel ($Mg yr^{-1}$); $RKLS_i$ = soil loss potential per pixel of the bare soil ($Mg yr^{-1}$); and SDR_{bar} = SDR for bare soil.

2.4. Data Sources and Processing

2.4.1. Cover-Management (C) and Support Practice (P) Factors

The land use and cover map for the year 2010, with a spatial resolution of 30 m, was obtained from Brazil MapBiomass collection 6 [40], through the Google Earth Engine platform [47] (Figure 3d). In this study, the C factor for each LULC condition in the present and prospective scenarios was obtained from the literature (Table 1). The P factor, representing the soil loss reduction provided by support practices, was taken as 1.0 for the calibration of the model [43].

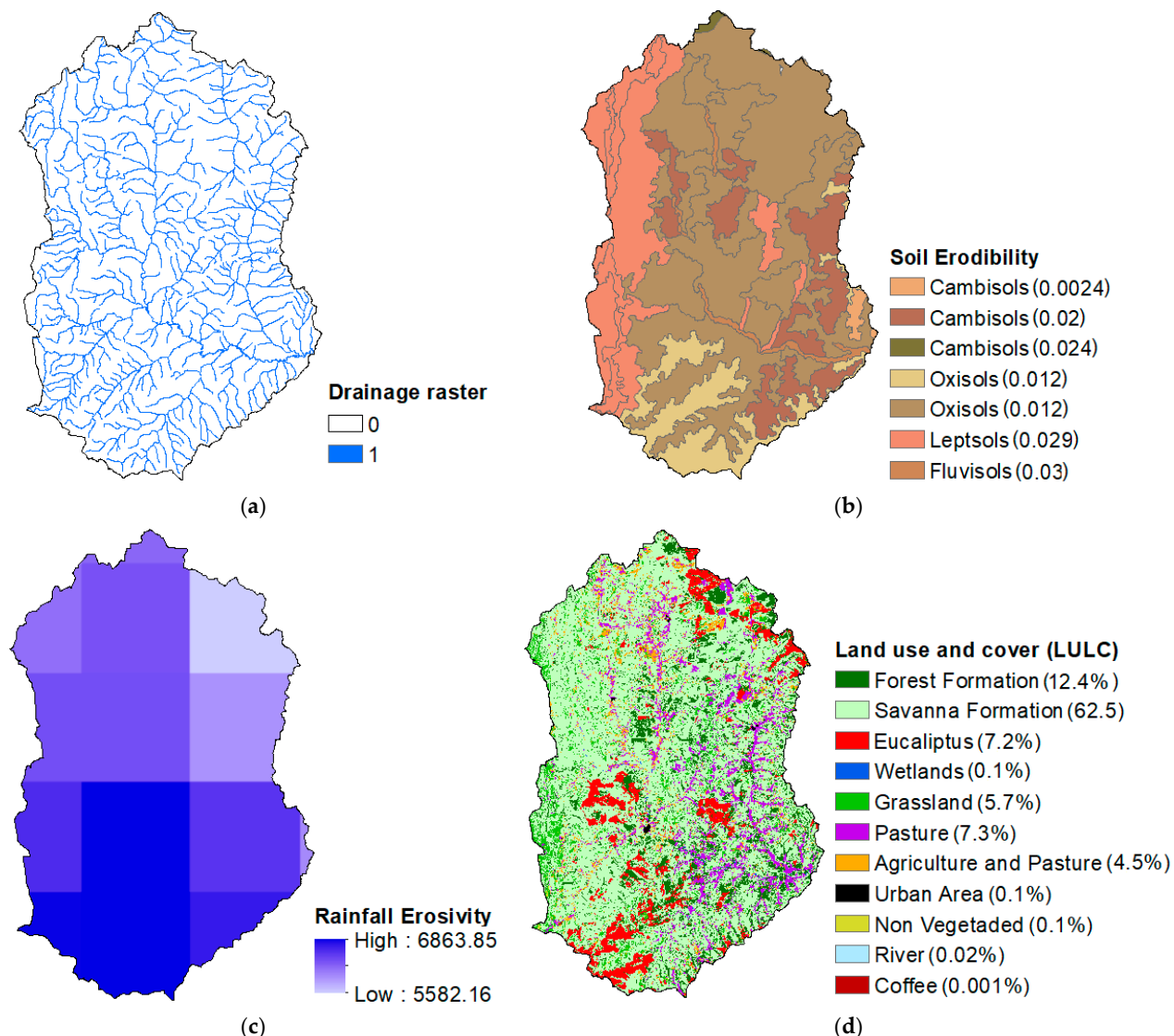


Figure 3. Inputs: Basin drainage (a); soils and soil erodibility (b); rainfall erosivity (c); and land use (d).

Table 1. Values of the cover-management factor (factor C) and the respective sources.

LULC	Factor C	Source
Native vegetation		
Forests Formation	0.004	[43,48]
Savanna Formation	0.012	[43,48]
Grassland	0.013	[43,48]
Wetlands	0	[43]
Anthropic areas		
Eucalyptus plantation	0.3	[49]
Pasture	0.035	[50]
Mosaic of Agriculture and Pasture	0.15	[50]
Coffee	0.11	[51]
Non vegetated *	1	[43]
Urban Area	0.03	[52]
Other		
Rocky Outcrop	0	[43]
River	0	[43]

2.4.2. Digital Elevation Model (DEM)

The digital elevation model (DEM) used was the SRTM-GL1 (version 3), with a spatial resolution of 30 m, obtained through the Google Earth Engine platform [47,53]. This DEM has less vertical bias and eliminates gaps and voids, making it reliable for regions of open savanna [54,55].

The SDR-InVEST model uses the DEM to determine the flow accumulation and the sediment flow path. In order to reduce topographic uncertainty, the basin DEM was corrected with a stream-burning technique [27,56], using the basin drainage network acquired by the Brazilian Institute of Geography and Statistics (IBGE) [57]. Drainage was converted from shapefile to grid format (raster). The “map processing extension” technique was used to extend the contour definitions of the drainage raster, based on the DEM extension, in the Arcgis 10.4.1 software. Subsequently, the extended drainage raster was used to correct the DEM. The drainage raster extended was also used as input data to represent the actual flow and to be merged into the simulated stream to ensure that the exported sediments were calculated correctly [27] (Figure 3a).

2.4.3. Rainfall Erosivity (R)

Basin rainfall erosivity (R), representing the potential of rainfall and runoff to cause soil erosion [43], was obtained using a Fournier-type equation [58] from monthly and annual precipitation data [37]:

$$R = 42.307 \cdot \left(\frac{M_p^2}{P_a} \right) + 69.763 \quad (14)$$

where R is the annual rainfall erosivity ($MJ \cdot mm(ha \cdot hr \cdot yr)^{-1}$); M_p is monthly precipitation (mm); and P_a is the annual precipitation (mm).

Precipitation data were obtained from the CHIRPS [59] satellite database for the period between 1985 and 2019 (Figure 3c). The CHIRPS monthly precipitation data were post-processed with a bias correction routine [60], using observed P data from three gauging stations as ground truth (Figure 1).

2.4.4. Soil Erodibility (K)

The soil erodibility factor (K) of basin soils (Figure 3b) was obtained by an equation developed for the Brazilian savanna [21]. The soil texture information for the equation was obtained from the BDIA platform, the Environmental Information Database (<https://bdiaweb.ibge.gov.br/>):

$$K = -0.000430 \cdot \left[\frac{(AF + SI)}{CO} \right] + 0.000437 * AT + 0.000863 \cdot SI \quad (15)$$

where AF = horizon sand content A; SI = silt content; CO = soil organic carbon content; and AT = total soil sand. The 1:250,000 scale soil map of the basin was obtained from the IBGE database [38].

2.5. Model Calibration

The threshold flow accumulation (TFA) parameter (2500) was obtained by comparing the synthetic stream network and drainage network in the real world through Google Earth [47,56]. The SDR-InVEST model was calibrated by adjusting the parameters L_{max} (the maximum allowed value of the slope length parameter (L), Equation (6)) and k (Equation (7)).

To evaluate the results simulated by the model, the simulated sediment annual yield (E_{sim}) at the basin outlet is compared to the observed sediment loading at the outlet of the watershed [MANUAL INVEST]. Thus, for each combination of these parameters, E_{sim}

was compared to the observed yield value, until a minimum percentage error (E_p) was obtained [61]:

$$E_p = \frac{\sum_{t=1}^n E_{\text{sim}} - \sum_{t=1}^n E_{\text{obs}}}{\sum_{t=1}^n E_{\text{obs}}} \cdot 100 \quad (16)$$

where E_{sim} is the simulated sediment yield (Mg yr^{-1}); E_{obs} is the observed sediment yield (obtained with the sediment rating curve—item 2.2) (Mg yr^{-1}). Model default values were used for the parameters SDRmax (0.8) and IC₀ (0.5).

2.6. Erosion, Sedimentation, and On- and Off-Site Soil Loss Tolerance

Mean soil loss (on-site erosion), calculated by the SDR-InVEST model, was compared to the on-site soil loss tolerance, taken as $10 \text{ Mg ha}^{-1} \text{yr}^{-1}$ [8,16,62], to obtain the basin areas with the risk of permanent degradation by erosion. With respect to sedimentation, the exported sediment in the basin pixels was compared with off-site tolerance, taken as $1.0 \text{ Mg ha}^{-1} \text{yr}^{-1}$ [18–20], above which the risk of sedimentation of the drainage channels is significant.

2.7. Simulation Scenarios

Different land use and climate scenarios were analyzed to assess erosion and sedimentation impacts, as well as basin sustainability with respect to on-site and off-site erosion and sedimentation tolerances.

- Land use Scenarios:

The land use/land cover LULC of 2010 was taken as the baseline condition (BL) (Figure 3). The pessimistic LULC scenario (PE) assumed that the anthropic areas (agriculture, pastures, eucalyptus, and non-vegetated areas) of the BL scenario were increased by 50% using the InVEST proximity-based model [27], which were added around the existing anthropic areas in the basin. Similarly, in the LULC optimistic scenario (OP), native vegetation replaced the original anthropic areas based on the remaining Cerrado vegetation of the baseline scenario using the proximity model.

- Conservation Scenarios

To estimate the impact of the Brazilian environmental legislation on the erosive and sediment retention processes in the basin, land conservation was established in the BL, OP, and PE scenarios (Land Use Scenarios—previous item), following the guidelines of the National System of Conservation Units (SNUC) [63] and the Brazilian Forest Code (CF) [64].

The implementation of CF guidelines consisted of the restoration of native vegetation in the areas of permanent preservation (APP) with anthropic use in 2010. Among the APPs indicated by the legislation, the following are considered here: 30 m-wide strips along drainage channels, 50 m at the headwater sources, and 100 m along the edges of plateaus.

The SNUC determines which uses and land cover are allowed for each category of Conservation Unit (UC). Thus, for the integral protection UC's (PEM and PESNT) (Figure 1), the anthropic areas in the inner limits were converted into native vegetation, and in the buffer zone (Figure 1), conservation practices (countering and terracing) were applied. For the UC of the sustainable development (RDSNG), conservation management practices were applied to anthropic areas in the inner limits and within the buffer zone of the UC (Figure 1).

The conservation management practices selected for the UCs were contouring and level terraces to minimize the erosion processes on steep slopes. This corresponded to a reduction of 50% in the original P factor (1.0) within the basin anthropic areas [43]. Thus, the BL_L (baseline LULC scenario and established land conservation (SNUC/CF)), OP_L (optimistic LULC scenario and established land conservation (SNUC/CF)), and PE_L (pessimistic LULC scenario and established land conservation (SNUC/CF)) scenarios were established.

- Climate change scenarios

Three climate scenarios were analyzed in the present study based on the erosivity mean and the standard deviation of the rainfall time series: (i) a baseline climate-Rm ($7336.3 \text{ MJ} \cdot \text{mm}(\text{ha} \cdot \text{hr} \cdot \text{yr})^{-1}$), using the mean annual erosivity of the period between 1985 and 2019; (ii) a dry climate-Rdry ($4944.4 \text{ MJ} \cdot \text{mm}(\text{ha} \cdot \text{hr} \cdot \text{yr})^{-1}$), reflecting the erosivity of a typical dry year (2008) of the historic series; and (iii) a wet climate-Rwet ($9874.7 \text{ MJ} \cdot \text{mm}(\text{ha} \cdot \text{hr} \cdot \text{yr})^{-1}$), represented by the erosivity of a typical wet year (2002).

3. Results

3.1. Sediment Rating Curve (SRC)

The sediment rating curve at the basin outlet is obtained from observed streamflow ($\text{m}^3 \text{ s}^{-1}$) and observed sediment load (t d^{-1}) with its respective power equation and the R^2 (Item 2.2. and Figure 4). The mean annual sediment yield, calculated based on the SRC equation, for the basin in the studied period was 13.1 Gg yr^{-1} .

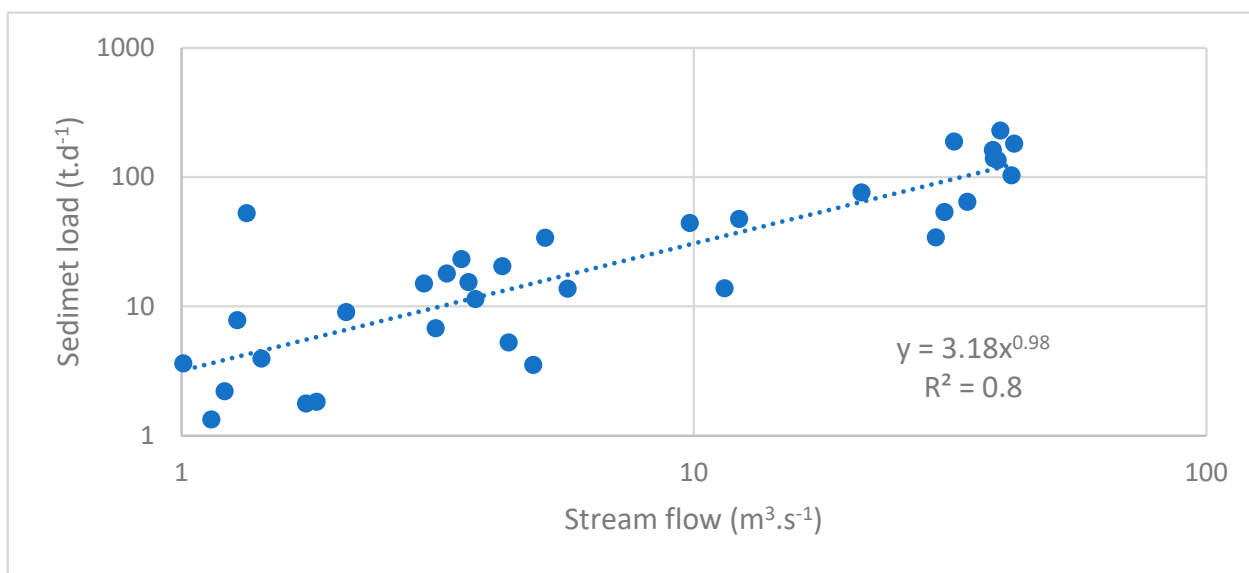


Figure 4. Sediment rating curve (SRC) in log scale.

3.2. Model Calibration

The calibrated values for parameters k and L_{\max} were 0.547 and 4.0, respectively, corresponding to a mean error of <1% between the simulated and observed sediment yield.

3.3. Model Simulation Scenarios

3.3.1. Soil Loss

Figure 5 shows the basin soil loss in the baseline; optimistic and pessimistic scenarios are very spatially variable.

In the different LULC scenarios, the mean soil loss ranged from $7 \text{ Mg ha}^{-1} \text{ yr}^{-1}$ for the OP_L scenario (Rdry) to $36 \text{ Mg ha}^{-1} \text{ yr}^{-1}$ for the PE scenario (Rwet) (Figure 6). The basin areas where erosion was above and below on-site soil loss tolerance are presented in Table 2 for the different land use, conservation, and climate scenarios.

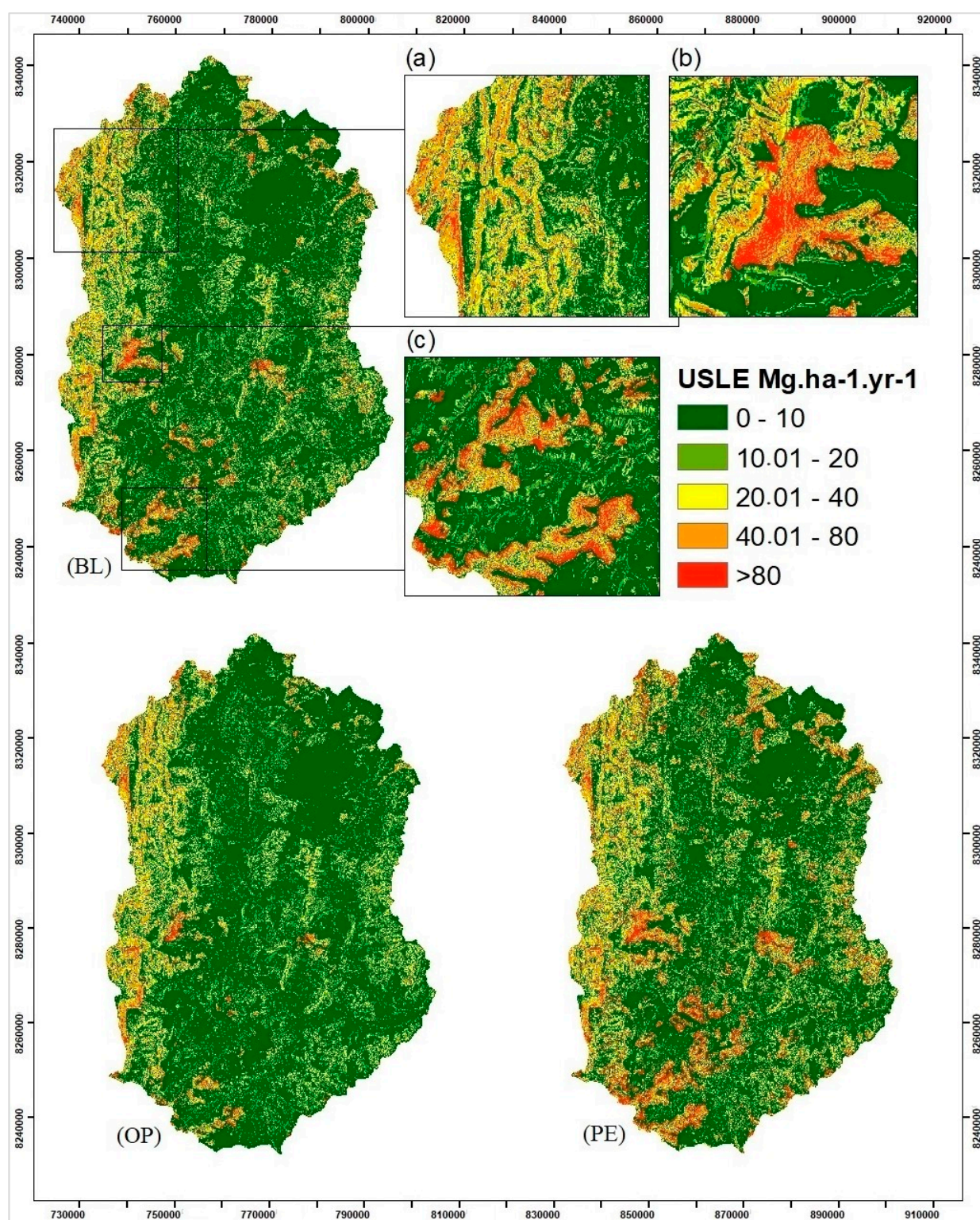


Figure 5. Basin soil loss (USLE) for the BL (baseline land use), the OP (optimistic land use), and the PE (pessimistic land use) scenarios, simulated with mean annual erosivity (baseline climate—Rm). The highlights of BL high erosion: (a) rugged slope, (b) eucalyptus plantation, and (c) eucalyptus plantations over highly erodible soils (Leptsols).



Figure 6. Mean basin soil loss. Land use scenarios: BL—baseline LULC, OP—optimistic LULC, and PE—pessimistic LULC; conservation scenarios: BL_L—baseline LULC and established land conservation, OP_L—optimistic LULC and established land conservation, and PE_L—pessimistic LULC and established land conservation; climate scenarios: Rm—baseline climate (mean erosivity), Rdry—dry climate, and RWET—wet climate.

Table 2. Percentage of basin areas with erosion above and below on-site soil loss tolerance ($10 \text{ Mg ha}^{-1} \text{ yr}^{-1}$) in the land use scenarios: BL—baseline LULC, OP—optimistic LULC, and PE—pessimistic LULC; conservation scenarios: BL_L—baseline LULC and established land conservation, OP_L—optimistic LULC and established land conservation, and PE_L—pessimistic LULC and established land conservation; climate scenarios: Rm—baseline climate (mean erosivity), Rdry—dry climate, and RWET—wet climate.

Scenarios	Rdry		Rm		RWET	
	$\leq T$	$> T$	$\leq T$	$> T$	$\leq T$	$> T$
OP	77.3	22.7	68.6	31.4	61.2	38.8
BL	71.8	28.2	62.7	37.3	55.2	44.8
PE	66.1	33.9	56.9	43.1	49.7	50.3
OP_L	80.0	20.0	72.0	28.0	64.8	35.2
BL_L	75.6	24.4	67.1	32.9	59.9	40.1
PE_L	71.1	28.9	62.5	37.5	55.4	44.6

3.3.2. Basin Sediment Yield and Exported Sediment

The annual basin sediment yield at the basin outlet varied from 0.2 to 0.3% and from 0.05 to 0.07% of the total soil loss generated inside the basin in the different LULC and conservation scenarios, respectively (Figure 7). The sediment yield ranged from 1.2 Gg yr^{-1} for the OP_L scenario (Rdry) to 52.2 Gg yr^{-1} for the PE scenario (RWET).

Table 3 presents the % of the basin areas where the exported sediment in the basin pixels were below and above the off-site tolerance threshold ($1.0 \text{ Mg ha}^{-1} \text{ yr}^{-1}$). A majority of the basin generates an amount of sediment below $1.0 \text{ Mg ha}^{-1} \text{ yr}^{-1}$, which reaches 100% in some scenarios (Table 3).

On average, only 0.1% of the basin area experienced off-site sedimentation above the tolerance threshold. Such areas were characterized by higher IC, SDR, CP, LS, K, R, and a slope grade above 20%, including mosaic of agriculture and pasture, deforested areas, and eucalyptus plantations. Conversely, the basin areas below the $1 \text{ Mg ha}^{-1} \text{ yr}^{-1}$ off-site tolerance threshold included natural forests, savannas, and pastureland in flatter areas.

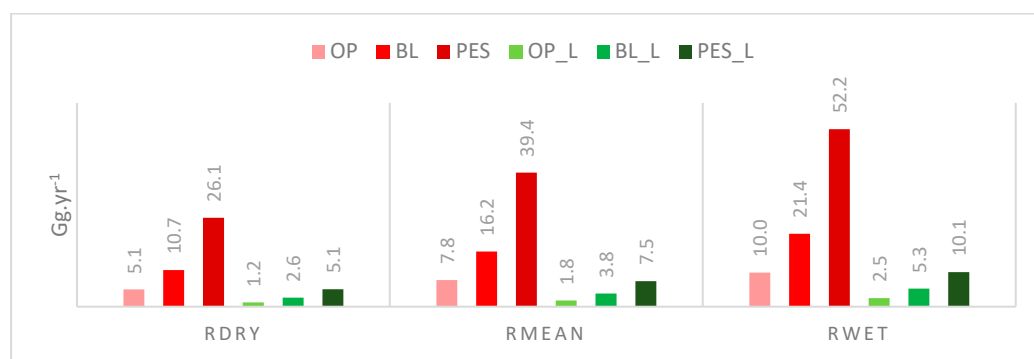


Figure 7. Total sediment yield at the basin outlet. Land use scenarios: BL—baseline LULC, OP—optimistic LULC, and PE—pessimistic LULC; conservation scenarios: BL_L—baseline LULC and established land conservation, OP_L—optimistic LULC and established land conservation, and PE_L—pessimistic LULC and established land conservation; climate scenarios: Rm—baseline climate (mean erosivity), Rdry—dry climate, and Rwet—wet climate.

Table 3. Percentage of the basin area above and below off-site sedimentation tolerance ($1 \text{ Mg ha}^{-1} \text{ yr}^{-1}$) in the land use scenarios: BL—baseline LULC, OP—optimistic LULC, and PE—pessimistic LULC; conservation scenarios: BL_L—baseline LULC and established land conservation, OP_L—optimistic LULC and established land conservation, and PE_L—pessimistic LULC and established land conservation; climate scenarios: Rm—baseline climate (mean erosivity), Rdry—dry climate, and Rwet—wet climate.

Scenarios	Rdry		Rm		Rwet	
	$\leq T$	$> T$	$\leq T$	$> T$	$\leq T$	$> T$
OP	99.99	0.01	99.94	0.06	99.93	0.07
BL	100.0	0.0	99.84	0.16	99.78	0.22
PE	100.0	0.0	99.42	0.58	99.16	0.84
OP_L	100.0	0.0	100.0	0.0	100.0	0.0
BL_L	100.0	0.0	99.99	0.01	99.98	0.02
PE_L	100.0	0.0	99.95	0.05	99.91	0.09

3.3.3. Sediment Retention

The results of sediment retention in the basin pixels are presented in Figure 8 for the different scenarios. According to that figure, little variation existed between the land use and conservation scenarios, but a significant difference in on-site sediment retention existed between the three climate (erosivity) scenarios.

3.3.4. Conservation Practices

In the different conservation scenarios, ecological restoration and conservation practices were applied to 10% of the basin area and reduced soil loss and sediment export (Table 4). The effectiveness of conservation measures was directly proportional to the increase in the anthropic area. In relation to the erosivity of the rain, this did not occur because in the Rwet scenario, the benefits were equal to or smaller than in the Rdry scenario.

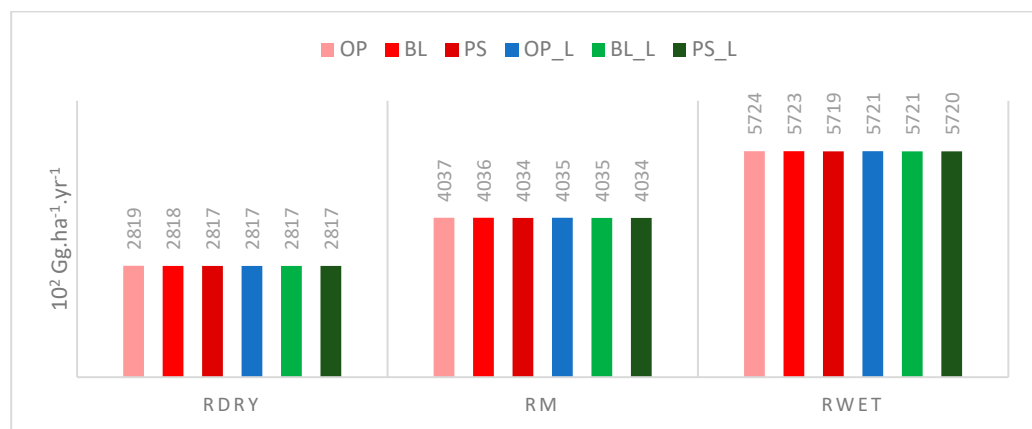


Figure 8. Total sediment retention in the basin (land use scenarios: BL—baseline LULC, OP—optimistic LULC, and PE—pessimistic LULC; conservation scenarios: BL_L—baseline LULC and established land conservation, OP_L—optimistic LULC and established land conservation, and PE_L—pessimistic LULC and established land conservation; climate scenarios: Rm—baseline climate (mean erosivity), Rdry—dry climate, and Rwet—wet climate).

Table 4. Percentage reduction in soil loss and sediment export after conservation practices. OP -> OP_L: land use scenario OP (optimistic LULC) to conservation scenario OP_L (optimistic LULC and established land conservation); BL -> BL_L: land use scenario BL (baseline LULC) to conservation scenario BL_L (baseline LULC and established land conservation); PE -> PE_L: land use scenario PE (pessimistic LULC) to conservation scenario PE_L (pessimistic LULC and established land conservation).

Variable & Scenario	Scenario Change		
	OP -> OP_L	BL -> BL_L	PE -> PE_L
Soil Loss	Rdry	19.6	22.8
	Rm	20.5	23.5
	Rwet	19.4	22.8
Sediment export	Rdry	75.8	75.4
	Rm	77.0	76.3
	Rwet	75.3	75.4

4. Discussion

4.1. Sediment Rating Curve (SRC)

The graphical and R2 results of the sediment rate curve of the Pardo-FB show a good fit [42]. However, there could be bias because of the low frequency of sediment sampling compared to stream flow [37].

4.2. Calibration Model

The low calibration (error < 1%) indicates that the InVEST-SDR model can explain the sedimentological behavior of the Pardo Basin, similar to findings of other studies in different parts of the world, using long-term data [23,30–34].

4.3. Soil Loss

The high soil loss rates ($>10 \text{ Mg ha}^{-1} \text{ yr}^{-1}$) in Figure 5 were associated with a combination of steep slopes, highly erodible soils, and anthropic land use. The values of soil loss increased on steep slopes, even though flat areas, where the conversion of the natural savanna into a mosaic of agriculture, pasture, and eucalyptus plantations, also had high values of soil loss, such as those found in other studies [3,7,10,46].

In the BL scenario with baseline erosivity, 63% of the basin area had erosion rates below the soil loss tolerance ($10 \text{ Mg ha}^{-1} \text{ yr}^{-1}$) (Figure 5). These areas are covered with

permanent vegetation (91%), areas of low steepness ($s < 10\%$), and areas of low erodibility ($K < 0.02$). The soil loss range between 10 and 80 $Mg\ ha^{-1}\ yr^{-1}$ (33% of the basin area) was dominated by land uses of permanent and non-permanent vegetation, steep slopes, and highly erodible soils ($K > 0.02$). Less than 4% of the basin area would experience severe erosion ($>80\ Mg\ ha^{-1}\ yr^{-1}$) in the BL scenario, which was associated with non-permanent vegetation, slopes $> 20\%$, and soil erodibility < 0.02 . The other LULC scenarios showed similar trends.

The differences in soil loss values among LULC types found a good correspondence with runoff plots in the Brazilian savanna, where soil losses from natural and undisturbed Cerrado conditions were very low compared to areas with conventional crops and forestry plantations [9,12,65–69]. The low soil loss rates of the native vegetation result from the permanent canopy and ground cover and the undisturbed, highly permeable soils, which facilitate the infiltration of water into the soil and reduce surface runoff [8,70–74].

The LULC changes increase the susceptibility to soil degradation mostly during the summer season, when intense precipitation events occur, such as in the Rwet scenario [10,23,43,66,75]. These justify the percentage of areas above tolerance for on-site soil loss, given the increase of anthropic areas and the extreme wet events found in the results.

4.4. Exported Sediment

Sediment export in the basin was directly proportional to rainfall erosivity and inversely correlated to permanent land cover, as reported in other studies [45,46]. In the scenario BL (Rm), anthropic areas contribute 6.4 times more than native vegetation to the total sediments that reach the basin outlet. The other scenarios showed similar trends.

Differences in sediment export among scenarios are influenced by sediment sources (soil loss) and by sediment delivery (soil loss delivery rate—SDR and continuity index—IC) [23,27,75–77]. Almost half of the agricultural and pasture mosaic areas are up to 130 m from the rivers in BL, and this increased in PE.

In these places, eroded sediments are less likely to find a sink to impede the sediment flow due to the proximity to rivers [23,75–77]. Furthermore, on the banks of rivers, the sediment loads, coming from slopes and more elevated areas, are potentially higher due to the greater distance and greater slope of the path [23,45,77].

The non-vegetated areas and eucalyptus plantations also occur close to rivers and in areas with slopes above 10%, which increases the susceptibility to sediment delivery [78]. In the OP scenario, sites close to rivers have a higher percentage of native vegetation, which provides greater impedance and infiltration of the water and eroded sediments [32,33,70,79,80].

It is inferred, then, that anthropic areas and their spatial distribution facilitate the transport of sediments from other parts of the basin to rivers. Thus, besides the increase in sediment sources, the expansion of anthropic areas over time enhances connectivity in the landscape, which results in a significant increase in sediment exports [23,45,75–77,81].

The chances of the soil particles being transported depend on the availability of water, which can be generated at the site and/or come from the slope [46]. Therefore, PE is a scenario that is not only pessimistic in relation to soil and water ecosystem services but also pessimistic in relation to climate change, favoring the negative effect of wet extremes.

4.5. Sediment Retention

The sediment retention was inversely proportional to soil loss and to the presence of permanent vegetation, unlike the results of similar studies [23,75,77]. The native vegetation has the potential to retain sediments, especially in the sloping areas, while deforested areas, coffee, and eucalyptus plantations showed the least sediment retention potential. Sediment retention was proportional to soil erosivity, a fact corroborated by other studies [10,23].

4.6. Land Conservation

The conservation practices used reduced impacts of the slope on soil water erosion and reduced the potential for sediment transport in the landscape and the delivery to rivers (SDR and CI) [40–46]. With less eroded sediments and low connectivity in the landscape, naturally the sediment export and areas above off-site tolerance will be reduced [13,37,38,47–49].

However, the results also showed that high rainfall scenarios limit the benefits of conservation practices. The vegetation's ability to influence soil loss and flow connectivity has strong temporal and spatial dynamics, which varies by seasons of the year and climatic extremes [16,46,82].

Borrelli et al. [3] simulated future changes in climate and land use in different parts of the world and observed that in scenarios of extreme humidity it will be necessary to expand the use of conservation practices and the restoration of native vegetation. However, the authors emphasize that for some locations, such practices may be insufficient to minimize the impacts of the intense erosivity of rainfall on erosion processes.

5. Conclusions

In the present (baseline) condition, the Pardo River basin has a mean soil loss of $19 \text{ Mg ha}^{-1} \text{yr}^{-1}$, equivalent to 1.9 times the on-site soil loss tolerance, as a consequence of non-permanent soil cover, steep slopes, and high soil erodibility. If unchecked, this could lead to permanent soil degradation.

Although the mean sediment exported from basin slopes exceeded the off-site sedimentation threshold in only 2% of the basin area, the high sediment yield at the basin outlet (a mean of 16.2 Gg yr^{-1}) has a high silting potential.

The results of the study indicate that permanent soil cover, reduced erosivity, and conservation practices significantly contribute to the reduction of on- and off-site soil loss impacts, such as land degradation and sedimentation, increasing the sediment retention on the basin slopes.

These findings, which were corroborated by other studies, could lead to the establishment of sound soil conservation policies in the Pardo basin and other similar watersheds of the Brazilian savanna, improving overall basin sustainability.

Author Contributions: Conceptualization, B.P.C.B. and H.M.L.C.; methodology, B.P.C.B. and H.M.L.C.; software, B.P.C.B. and H.M.L.C.; validation, B.P.C.B., H.M.L.C. and A.S.; investigation, B.P.C.B. and H.M.L.C.; data curation, B.P.C.B., H.M.L.C. and A.S.; writing—original draft preparation, B.P.C.B., H.M.L.C. and A.S.; writing—review and editing, B.P.C.B., H.M.L.C. and A.S.; funding acquisition, B.P.C.B., H.M.L.C. and A.S. All authors have read and agreed to the published version of the manuscript.

Funding: This research was supported by the Brazilian Agricultural Research Corporation (Embrapa), United Nations Development Programme (UNDP) and Global Environment Facility (GEF) provided financial support through the Bem Diverso Project (Project BRA/14/G33); and The APC was funded by the Postgraduate Department of the University of Brasilia (UnB).

Data Availability Statement: The streamflow, concentration of suspended solids and observed precipitation data are available at <<https://www.snirh.gov.br/hidroweb>>, CHIRPS data at <<https://www.chc.ucsb.edu/data/chirps>>, land-use data at <<http://mapbiomas.org/>>, soil data at <<https://www.ibge.gov.br/geociencias/cartas-e-mapas/informacoes-ambientais/15842-biomas.html?edicao=16060&rt=acesso-ao-produto>>, <<https://bdiaweb.ibge.gov.br>> and DEM data at <https://developers.google.com/earth-engine/datasets/catalog/USGS_SRTMGL1_003>. Data were accessed between August 2021 and June 2022.

Conflicts of Interest: The authors declare no conflict of interest.

References

- FAO. *Healthy Soils Are the Basis for Healthy Food Production*; FAO: Rome, Italy, 2015.
- Montanarella, L. Agricultural Policy: Govern Our Soils. *Nature* **2015**, *528*, 32–33. [[CrossRef](#)]

3. Borrelli, P.; Robinson, D.A.; Panagos, D.P.; Lugato, E.; Yang, J.E.; Alewell, C.; Wuepper, D.; Montanarella, L.; Ballabio, C. Land Use and Climate Change Impacts on Global Soil Erosion by Water (2015–2070). *Proc. Natl. Acad. Sci. USA* **2020**, *117*, 21994–22001. [[CrossRef](#)]
4. Kosmus, M.; Renner, I.; Ullrich, S. *Integração de Serviços Ecossistêmicos Ao Planejamento Do Desenvolvimento*; Deutsche Gesellschaft für Internationale Zusammenarbeit (GIZ) GmbH: Bonn, Germany, 2012.
5. Alewell, C.; Borrelli, P.; Meusburger, K.; Panagos, P. Using the USLE: Chances, Challenges and Limitations of Soil Erosion Modelling. *Int. Soil Water Conserv. Res.* **2019**, *7*, 203–225. [[CrossRef](#)]
6. Anache, J.A.A.; Wendland, E.C.; Oliveira, P.T.S.; Flanagan, D.C.; Nearing, M.A. Runoff and Soil Erosion Plot-Scale Studies under Natural Rainfall: A Meta-Analysis of the Brazilian Experience. *Catena* **2017**, *152*, 29–39. [[CrossRef](#)]
7. Gomes, L.; Simões, S.; Dalla Nora, E.; de Sousa-Neto, E.; Forti, M.; Ometto, J. Agricultural Expansion in the Brazilian Cerrado: Increased Soil and Nutrient Losses and Decreased Agricultural Productivity. *Land* **2019**, *8*, 12. [[CrossRef](#)]
8. Fonseca, M.R.S.; Uagoda, R.; Chaves, H.M.L. Rates, Factors, and Tolerances of Water Erosion in the Cerrado Biome (Brazil): A Meta-analysis of Runoff Plot Data. *Earth Surf. Process. Land.* **2022**, *47*, 582–595. [[CrossRef](#)]
9. Rieger, F.A.; Zolin, C.A.; Paulino, J.; de Souza, A.P.; da Matos, E.S.; de Souza Magalhães, C.A.; de Farias Neto, A.L. Water Erosion on an Oxisol under Integrated Crop-Forest Systems in a Transitional Area between the Amazon and Cerrado Biomes. *Rev. Bras. Cienc. Solo* **2016**, *40*, 1–12. [[CrossRef](#)]
10. Perović, V.; Kadović, R.; Djurdjević, V.; Braunović, S.; Čakmak, D.; Mitrović, M.; Pavlović, P. Effects of Changes in Climate and Land Use on Soil Erosion: A Case Study of the Vranjska Valley, Serbia. *Reg. Environ. Change* **2019**, *19*, 1035–1046. [[CrossRef](#)]
11. Marengo, J.A.; Cunha, A.P.; Alves, L.M. *Variabilidade e Mudanças Climáticas No Semiárido Brasileiro*; Instituto Nacional do Semiárido: Campina Grande, Brazil, 2016; Volume 1.
12. Anache, J.A.A.; Flanagan, D.C.; Srivastava, A.; Wendland, E.C. Land Use and Climate Change Impacts on Runoff and Soil Erosion at the Hillslope Scale in the Brazilian Cerrado. *Sci. Total Environ.* **2018**, *622–623*, 140–151. [[CrossRef](#)]
13. de Oliveira Ferreira, V. Unidades de Paisagem Da Bacia Do Rio Jequitinhonha, Em Minas Gerais: Subsídios Para a Gestão de Recursos Hídricos. *Caminhos Geogr.* **2011**, *12*, 239–257. [[CrossRef](#)]
14. Rodriguez Sousa, A.A.; Muñoz-Rojas, J.; Pinto-Correia, T.; Aguilera, P.A.; Barandica, J.M.; Rescia, A.J. A Comparative Analysis of Soil Loss Tolerance and Productivity of the Olive Groves in the Protected Designation of Origin (PDO) Areas Norte Alentejano (Portugal) and Estepa (Andalusia, Spain). *Agronomy* **2021**, *11*, 665. [[CrossRef](#)]
15. Schertz, D.L. The Basis for Soil Loss Tolerances. *J. Soil Water Conserv. Jan.* **1983**, *38*, 10–14.
16. Bertoni, J.; Neto, F.L. *Conservação Do Solo*, 9th ed.; Ícone: São Paulo, Brazil, 2014.
17. Fox, G.A.; Sheshukov, A.; Cruse, R.; Kolar, R.L.; Guertault, L.; Gesch, K.R.; Dutnall, R.C. Reservoir Sedimentation and Upstream Sediment Sources: Perspectives and Future Research Needs on Streambank and Gully Erosion. *Environ. Manag.* **2016**, *57*, 945–955. [[CrossRef](#)]
18. Morgan, R.P.C.S. *Soil Erosion and Conservation*, 3rd ed.; National Soil Resources Institute, Cranfield University: Bedford, UK, 2005.
19. Verheijen, F.G.A.; Jones, R.J.A.; Rickson, R.J.; Smith, C.J. Tolerable versus Actual Soil Erosion Rates in Europe. *Earth Sci. Rev.* **2009**, *94*, 23–38. [[CrossRef](#)]
20. Moldenhauer, W.C.; Onstad, C.A. Achieving Specified Soil Loss Levels. *J. Soil Water Conserv.* **1975**, *30*, 166–168.
21. Chaves, H.M.L.; Piau, L.P. Efeito Da Variabilidade Da Precipitação Pluvial e Do Uso e Manejo Do Solo Sobre o Escoamento Superficial e o Aporte de Sedimento de Uma Bacia Hidrográfica Do Distrito Federal. *Rev. Bras. Cienc. Solo* **2008**, *32*, 333–343. [[CrossRef](#)]
22. Da Silva, C.R.; Chaves, H.M.L.; Camelo, A.P. Calibração e Validação Da Equação Universal de Perda de Solos Modificada (MUSLE) Utilizando Dados Hidrossedimentológicos Locais. *Rev. Bras. Cienc. Solo* **2011**, *35*, 1431–1439. [[CrossRef](#)]
23. Terrado, M.; Acuña, V.; Ennaanay, D.; Tallis, H.; Sabater, S. Impact of Climate Extremes on Hydrological Ecosystem Services in a Heavily Humanized Mediterranean Basin. *Ecol. Indic.* **2014**, *37*, 199–209. [[CrossRef](#)]
24. Robinson, D.A.; Panagos, P.; Borrelli, P.; Jones, A.; Montanarella, L.; Tye, A.; Obst, C.G. Soil Natural Capital in Europe; a Framework for State and Change Assessment. *Sci. Rep.* **2017**, *7*, 6706. [[CrossRef](#)]
25. Croke, J.; Nethery, M. Modelling Runoff and Soil Erosion in Logged Forests: Scope and Application of Some Existing Models. *Catena* **2006**, *67*, 35–49. [[CrossRef](#)]
26. Chaves, H.M.L.; Nearing, M.A. Uncertainty Analysis of the WEPP Soil Erosion Model. *Trans. ASAE* **1991**, *34*, 2437–2444. [[CrossRef](#)]
27. Sharp, R.; Douglass, J.; Wolny, S.; Arkema, K.; Bernhardt, J.; Bierbower, W.; Chaumont, N.; Denu, D.; Fisher, D.; Glowinski, K.; et al. *InVEST 3.11.0. User's Guide*; Stanford University: Stanford, CA, USA, 2020.
28. Da Cunha, E.R.; Santos, C.A.G.; da Silva, R.M.; Panachuki, E.; de Oliveira, P.T.S.; de Oliveira, N.S.; dos Falcão, K.S. Assessment of Current and Future Land Use/Cover Changes in Soil Erosion in the Rio Da Prata Basin (Brazil). *Sci. Total Environ.* **2022**, *818*, 151811. [[CrossRef](#)]
29. da Anjinho, P.S.; Barbosa, M.A.G.A.; Mauad, F.F. Evaluation of InVEST's Water Ecosystem Service Models in a Brazilian Subtropical Basin. *Water* **2022**, *14*, 1559. [[CrossRef](#)]
30. Hamel, P.; Chaplin-Kramer, R.; Sim, S.; Mueller, C. A New Approach to Modeling the Sediment Retention Service (InVEST 3.0): Case Study of the Cape Fear Catchment, North Carolina, USA. *Sci. Total Environ.* **2015**, *524–525*, 166–177. [[CrossRef](#)]
31. Pavani, B.F.; Ribeiro, T.C.L.; Gonçalves, D.A.; de Sousa Júnior, W.C.; Giarolla, A.; Arraut, E.M. Payments for Ecosystem Services to Water Resources Protection in Paraíba Do Sul Environmental Protection Area. *Ambiente Soc.* **2020**, *23*, 1–24. [[CrossRef](#)]

32. Saad, S.I.; Mota da Silva, J.; Ponette-González, A.G.; Silva, M.L.N.; da Rocha, H.R. Modeling the On-Site and off-Site Benefits of Atlantic Forest Conservation in a Brazilian Watershed. *Ecosyst. Serv.* **2021**, *48*, 101260. [CrossRef]
33. Saad, S.I.; Mota da Silva, J.; Silva, M.L.N.; Guimarães, J.L.B.; Sousa Júnior, W.C.; de Figueiredo, R.O.; da Rocha, H.R. Analyzing Ecological Restoration Strategies for Water and Soil Conservation. *PLoS ONE* **2018**, *13*, e0192325. [CrossRef]
34. Hamel, P.; Valencia, J.; Schmitt, R.; Shrestha, M.; Piman, T.; Sharp, R.P.; Francesconi, W.; Guswa, A.J. Modeling Seasonal Water Yield for Landscape Management: Applications in Peru and Myanmar. *J. Environ. Manage.* **2020**, *270*, 110792. [CrossRef]
35. Risso, L.M.; Nearing, M.A.; Laflen, J.M.; Nicks, A.D. Error Assessment in the Universal Soil Loss Equation. *Soil Sci. Soc. Am. J.* **1993**, *57*, 825–833. [CrossRef]
36. IBGE. IBGE Cidades. Available online: <https://cidades.ibge.gov.br/> (accessed on 31 January 2022).
37. de Carvalho, O.C. *Hidrossedimentologia Prática*, 2nd ed.; CPRM: Rio de Janeiro, Brazil, 2008.
38. IBGE—Informações Ambientais. Available online: <https://www.ibge.gov.br/geociencias/cartas-e-mapas/informacoes-ambientais/15842-biomas.html?edicao=16060&t=acesso-ao-produto> (accessed on 31 January 2022).
39. IBGE. Semiárido Brasileiro. Available online: <https://www.ibge.gov.br/geociencias/cartas-e-mapas/mapas-regionais/15974-semiarido-brasileiro.html> (accessed on 27 September 2021).
40. Souza, C.M.; Shimbo, J.Z.; Rosa, M.R.; Parente, L.L.; Alencar, A.A.; Rudorff, B.F.T.; Hasenack, H.; Matsumoto, M.; Ferreira, L.G.; Souza-Filho, P.W.M.; et al. Reconstructing Three Decades of Land Use and Land Cover Changes in Brazilian Biomes with Landsat Archive and Earth Engine. *Remote Sens.* **2020**, *12*, 2735. [CrossRef]
41. ANA—Agência Nacional de Águas. *Hidroweb: Sistemas de Informações Hidrológicas*; ANA—Agência Nacional de Águas: Brasilia, Brazil, 2018.
42. Lima, J.E.F.W.; Lopes, W.T.A.; de Carvalho, N.O.; da Silva, E.M.; Vieira, M.R. Fluxo de Sedimentos Em Suspensão No Exutório de Grandes Bacias Hidrográficas Em Território Brasileiro. In Proceedings of the VII Encontro Nacional de Engenharia de Sedimentos, Porto Alegre, Brazil, 20–24 November 2006.
43. Wischmeier, W.H.; Smith, D.D. *Predicting Rainfall Erosion Losses: A Guide to Conservation Planning*; USDA: Washington, DC, USA, 1978.
44. Desmet, P.J.J.; Govers, G. A GIS Procedure for Automatically Calculating the USLE LS Factor on Topographically Complex Landscape Units. *J. Soil* **1996**, *51*, 427–433.
45. Vigiak, O.; Borselli, L.; Newham, L.T.H.; McInnes, J.; Roberts, A.M. Comparison of Conceptual Landscape Metrics to Define Hillslope-Scale Sediment Delivery Ratio. *Geomorphology* **2012**, *138*, 74–88. [CrossRef]
46. Borselli, L.; Cassi, P.; Torri, D. Prolegomena to Sediment and Flow Connectivity in the Landscape: A GIS and Field Numerical Assessment. *Catena* **2008**, *75*, 268–277. [CrossRef]
47. Gorelick, N.; Hancher, M.; Dixon, M.; Ilyushchenko, S.; Thau, D.; Moore, R. Google Earth Engine: Planetary-Scale Geospatial Analysis for Everyone. *Remote Sens. Environ.* **2017**, *202*, 18–27. [CrossRef]
48. Righetto, A.M. *Hidrologia e Recursos Hídricos*; EESC-USP: São Paulo, Brazil, 1998.
49. Martins, S.G.; Silva, M.L.N.; Avanzi, J.C.; Curi, N.; Fonseca, S. Fator Cobertura e Manejo Do Solo e Perdas de Solo e Água Em Cultivo de Eucalipto e Em Mata Atlântica Nos Tabuleiros Costeiros Do Estado Do Espírito Santo. *Sci. For.* **2010**, *38*, 517–526.
50. Dos Santos, J.C.N.; de Andrade, E.M.; Medeiros, P.H.A.; de Araújo Neto, J.R.; de Palácio, H.A.Q.; do Rodrigues, R.N. Determination of the Cover Factor and the MUSLE Coefficients in Watersheds in the Brazilian Semiarid Region. *Rev. Bras. De Eng. Agric. E Ambient.* **2014**, *18*, 1157–1164. [CrossRef]
51. Prochnow, D.; Dechen, S.C.F.; de Maria, I.C.; de Castro, O.M.; Vieira, S.R. Razão de Perdas de Terra e Fator C Da Cultura Do Cafeiro Em Cinco Espaçamentos, Em Pindorama (SP). *Rev. Bras. Cienc. Solo* **2005**, *29*, 91–98. [CrossRef]
52. IGAM. *Plano Diretor de Recursos Hídricos Dos Afluentes Mineiros Do Rio Pardo_PA1*; IGAM: Belo Horizonte, Brazil, 2011.
53. Farr, T.G.; Rosen, P.A.; Caro, E.; Crippen, R.; Duren, R.; Hensley, S.; Kobrick, M.; Paller, M.; Rodriguez, E.; Roth, L.; et al. The Shuttle Radar Topography Mission. *Rev. Geophys.* **2007**, *45*, RG2004. [CrossRef]
54. Orlandi, A.G.; de Carvalho, O.A., Jr.; Guimarães, R.F.; Bias, E.d.S.; Corrêa, D.C.; Gomes, R.A.T. Vertical Accuracy Assessment of the Processed Srtm Data for the Brazilian Territory. *Bol. Ciências Geodésicas* **2019**, *25*, 1–14. [CrossRef]
55. Costa, C.A.G.; dos Teixeira, A.S.; de Andrade, E.M.; de Lucena, A.M.P.; de Castro, M.A.H. Análise Da Influência Vegetacional Na Altimetria Dos Dados SRTM Em Bacias Hidrográficas No Semiárido. *Rev. Ciência Agronômica* **2010**, *41*, 222–230. [CrossRef]
56. Maidment, D. *Handbook of Hydrology*; McGraw-Hill Education: New York, NY, USA, 1993.
57. IBGE. Bases Cartográficas Contínuas. Available online: <https://www.ibge.gov.br/geociencias/cartas-e-mapas/bases-cartograficas-continuas/15759-brasil.html?=&t=acesso-ao-produto> (accessed on 27 April 2022).
58. Da Silva, A.M. Rainfall Erosivity Map for Brazil. *Catena* **2004**, *57*, 251–259. [CrossRef]
59. De Sousa, K.; Sparks, A.H.; Ashmall, W.; van Etten, J.; Solberg, S.Ø. Chirps: API Client for the CHIRPS Precipitation Data in R. *J. Open Source Softw.* **2020**, *5*, 2419. [CrossRef]
60. Gudmundsson, L.; Bremnes, J.B.; Haugen, J.E.; Engen-Skaugen, T. Technical Note: Downscaling RCM Precipitation to the Station Scale Using Statistical Transformations—A Comparison of Methods. *Hydrol. Earth Syst. Sci.* **2012**, *16*, 3383–3390. [CrossRef]
61. Sarmento, L. Análise de Incertezas e Avaliação Dos Fatores Influentes No Desempenho de Modelos de Simulação de Bacias Hidrográficas. Ph.D. Thesis, University of Brasilia, Brasilia, Brazil, 2010.
62. Chaves, H.M.L. Incertezas Na Predição Da Erosão Com a USLE: Impactos e Mitigação. *Rev. Bras. Ciência Solo* **2010**, *34*, 2021–2029. [CrossRef]

63. BRASIL SNUC—Sistema Nacional de Unidades de Conservação Da Natureza. *Lei No 9.985*; BRASIL SNUC: Brasilia, Brazil , 2000.
64. BRASIL Código Florestal. *Lei No 12.651*; BRASIL Código Florestal: Brasilia, Brazil , 2012.
65. Oliveira, P.T.S.; Nearing, M.A.; Wendland, E. Orders of Magnitude Increase in Soil Erosion Associated with Land Use Change from Native to Cultivated Vegetation in a Brazilian Savannah Environment. *Earth Surf. Process Landf.* **2015**, *40*, 1524–1532. [[CrossRef](#)]
66. Anache, J.A.A. Alterações No Ciclo Hidrológico e Na Perda de Solo Devido Aos Diferentes Usos Do Solo e Variações Climáticas Em Área de Cerrado. Ph.D. Thesis, Universidade de São Paulo, São Paulo, Brazil, 2017.
67. Cândido, B.M.; Silva, M.L.N.; Curi, N.; Batista, P.V.G. Erosão Hídrica Pós-Plantio Em Florestas de Eucalipto Na Bacia Do Rio Paraná, No Leste Do Mato Grosso Do Sul. *Rev. Bras. Cienc. Solo* **2014**, *38*, 1565–1575. [[CrossRef](#)]
68. Carvalho, R.; Silva, M.L.N.; Avanzi, J.C.; Curi, N.; Souza, F.S. de Erosão Hídrica Em Latossolo Vermelho Sob Diversos Sistemas de Manejo Do Cafeiro No Sul de Minas Gerais. *Ciência Agropecuária* **2007**, *31*, 1679–1687. [[CrossRef](#)]
69. Pires, L.S.; Silva, M.L.N.; Curi, N.; Leite, F.P.; Brito, L.d.F. Erosão Hídrica Pós-Plantio Em Florestas de Eucalipto Na Região Centro-Leste de Minas Gerais. *Pesqui. Agropecu. Bras.* **2006**, *41*, 687–695. [[CrossRef](#)]
70. Sano, S.M.; de Almeida, S.P.; Ribeiro, J.F. *Cerrado: Ecologia e Flora*; Embrapa Cerrados: Brasilia, Brazil, 2018; Volume 1.
71. Da Silva, P.C.G.; de Moura, M.S.B.; Kiill, L.H.P.; de Brito, L.T.L.; Pereira, L.A.; Sá, I.B.; Correia, R.C.; de Teixeira, A.H.C.; Cunha, T.J.F.; Guimarães Filho, C. Caracterização Do Semiárido Brasileiro: Fatores Naturais e Humanos. In *Semiárido Brasileiro: Pesquisa, Desenvolvimento e Inovação*; Embrapa Semiárido; Embrapa Semiárido: Petrolina, Brazil, 2010.
72. Lima, J.E.F.W.; Silva, M.d.S. Estimativa Da Contribuição Hídrica Do Cerrado Para As Grandes Bacias Hidrográficas Brasileiras. In Proceedings of the XVII Simpósio Brasileiro de Recursos Hídricos, Associação Brasileira de Recursos Hídricos. São Paulo, Brazil, 25–29 November 2007; pp. 1–15.
73. Lima, J.E.F.W. Modelagem Numérica Do Fluxo Da Água No Solo e Do Escoamento de Base Em Uma Bacia Experimental Em Área Agrícola No Cerrado (Distrito Federal). Ph.D. Thesis, Universidade de Brasília, Brasilia, Brazil, 2010.
74. Gmach, M.-R.; Dias, B.O.; Silva, C.A.; Nóbrega, J.C.A.; Lustosa-Filho, J.F.; Siqueira-Neto, M. Soil Organic Matter Dynamics and Land-Use Change on Oxisols in the Cerrado, Brazil. *Geoderma Reg.* **2018**, *14*, e00178. [[CrossRef](#)]
75. Vaughan, A.A.; Belmont, P.; Hawkins, C.P.; Wilcock, P. Near-Channel Versus Watershed Controls on Sediment Rating Curves. *J. Geophys. Res. Earth Surf.* **2017**, *122*, 1901–1923. [[CrossRef](#)]
76. Zhou, M.; Deng, J.; Lin, Y.; Belete, M.; Wang, K.; Comber, A.; Huang, L.; Gan, M. Identifying the Effects of Land Use Change on Sediment Export: Integrating Sediment Source and Sediment Delivery in the Qiantang River Basin, China. *Sci. Total Environ.* **2019**, *686*, 38–49. [[CrossRef](#)] [[PubMed](#)]
77. Jamshidi, R.; Dragovich, D.; Webb, A.A. Distributed Empirical Algorithms to Estimate Catchment Scale Sediment Connectivity and Yield in a Subtropical Region. *Hydrol. Process* **2014**, *28*, 2671–2684. [[CrossRef](#)]
78. Wischmeier, W.A. Use and Misuse of the USLE. *J. Soiland Water Conserv.* **1976**, *31*, 5–9.
79. Durigan, G.; Munhoz, C.B.; Zakia, M.J.B.; Oliveira, R.S.; Pilon, N.A.L.; do Valle, R.S.T.; Walter, B.M.T.; Honda, E.A.; Pott, A. Cerrado Wetlands: Multiple Ecosystems Deserving Legal Protection as a Unique and Irreplaceable Treasure. *Perspect. Ecol. Conserv.* **2022**, *20*, 185–196. [[CrossRef](#)]
80. Thellmann, K. Simulating the Impact of Land Use Change and Climate Change on the Supply of Ecosystem Services in a Rubber-Dominated Watershed in Southwestern China. Ph.D. Thesis, University of Honenheim, Stuttgart-Hohenheim, Germany, 2020.
81. Gashaw, T.; Bantider, A.; Zeleke, G.; Alamirew, T.; Jemberu, W.; Worqlul, A.W.; Dile, Y.T.; Bewket, W.; Meshesha, D.T.; Adem, A.A.; et al. Evaluating InVEST Model for Estimating Soil Loss and Sediment Export in Data Scarce Regions of the Abbay (Upper Blue Nile) Basin: Implications for Land Managers. *Environ. Chall.* **2021**, *5*, 100381. [[CrossRef](#)]
82. Ben Zaied, M.; Jomaa, S.; Ouessar, M. Soil Erosion Estimates in Arid Region: A Case Study of the Koutine Catchment, Southeastern Tunisia. *Appl. Sci.* **2021**, *11*, 6763. [[CrossRef](#)]

Disclaimer/Publisher’s Note: The statements, opinions and data contained in all publications are solely those of the individual author(s) and contributor(s) and not of MDPI and/or the editor(s). MDPI and/or the editor(s) disclaim responsibility for any injury to people or property resulting from any ideas, methods, instructions or products referred to in the content.